

See discussions, stats, and author profiles for this publication at:
<http://www.researchgate.net/publication/237501538>

Compositional Variations in Smectites. Part II: Alteration of Acidic Precursors, A Case Study from Milos Island, Greece

ARTICLE *in* CLAY MINERALS · JANUARY 1997

Impact Factor: 0.97 · DOI: 10.1180/claymin.1997.032.2.07

CITATIONS

34

READS

24

2 AUTHORS, INCLUDING:



[G.E. Christidis](#)

Technical University of Crete

48 PUBLICATIONS 690 CITATIONS

SEE PROFILE

Compositional variations in smectites. Part II: alteration of acidic precursors, a case study from Milos Island, Greece

G. CHRISTIDIS AND A. C. DUNHAM*

Technical University of Crete, Department of Mineral Resources Engineering, 73133 Chania, Greece and

**Department of Geology, University of Leicester, University Road, Leicester, LE1 7RH, UK*

(Received 14 October 1992; revised 30 July 1996)

ABSTRACT: The smectites present in some bentonites from the Island of Milos, Greece, derived from acidic rocks, have been examined by XRD and electron microprobe. The possible influence of loss of alkalis during analysis and contamination by fine grained Si-phases on microanalyses has also been evaluated. Smectites are closely associated with opal-CT and their composition ranges from beidellite to Tatatilla-type montmorillonite. Their chemistry is dominated by negative relationships between Mg and Al^{VI} and Si and total Al. However, it cannot be resolved whether there is a solid-solution between the smectites or whether the variation observed is due to mechanical mixing of domains with different composition. The role of Fe is of minor importance reflecting an inherited factor imposed by the parent rock, but the role of the fluid phase is also important. Beidellite occurs in the rims, while Tatatilla-type montmorillonite, often associated with free opal-CT, is formed in the interior of the altered shards, indicating a variable degree of Si release during glass dissolution. The formation of beidellite is not necessarily associated with Mg uptake.

The compositional and structural heterogeneity of smectites has been studied thoroughly in the past (Tettenhorst & Johns, 1966; Stul & Mortier, 1974; Lagaly & Weiss, 1975; Lagaly *et al.*, 1976; Goulding & Talibudeen, 1980; Paquet *et al.*, 1982; Talibudeen & Goulding, 1983; Nadeau *et al.*, 1985; Lim & Jackson, 1986; Decarreau *et al.*, 1987; Goodman *et al.*, 1988; Iwasaki & Watanabe, 1988; Banfield & Eggleton, 1990; Banfield *et al.*, 1991a,b among others). Although the existence of compositional heterogeneity in Al-rich smectites is well known, the factors which control it are not well understood. Weaver & Pollard (1973) assumed a complete solid-solution between beidellite and montmorillonite, but Brigatti & Poppi (1981) Köster (1982) and Yamada *et al.* (1991) rejected this possibility. Brigatti & Poppi (1981) considered the existence of solid-solutions between the montmorillonite species. Previously, Grim & Kulbicki (1961) had proposed that Wyoming-type and Cheto-type montmorillonites do not form any

kind of solid-solution. Decarreau *et al.* (1987) suggested the existence of layers or domains of different composition in Ni-Fe-Mg smectites from lateritic profiles. Finally Meunier & Velde (1989) considered a solid-solution between high- and low-charged montmorillonite but not between montmorillonite and beidellite.

In a previous paper, Christidis & Dunham (1993) showed that the bentonites derived from intermediate (dacitic-andesitic) precursors, are extremely heterogeneous, as far as smectite composition is concerned. They reported the existence of a compositional transition between beidellite and Tatatilla-type (Cheto) montmorillonite, suggesting the possibility of a solid-solution between the two species. In contrast, no transition was observed either between beidellite and Wyoming-type montmorillonite or between Cheto-type- and Wyoming-type montmorillonite. This study examines smectites derived from acidic rocks and its purpose is to: (a) discuss possible chemical factors

which control the genesis of smectites during alteration of acidic rocks; (b) shed more light on the compositional transitions between the various smectite species; and (c) investigate the possible role of the nature of the parent rock on: (i) the type of the smectite formed; (ii) the compositional trends observed; and (iii) the physical properties of bentonites.

bentonite deposits studied are located in the Komia area, Eastern Milos (Fig. 1). The geological features and genesis of the bentonites have been described by Christidis *et al.* (1995). All deposits have been affected by hydrothermal alteration which is a later event and is associated with the replacement of smectite by kaolinite, and deposition of carbonates and sulphates (Christidis, 1992; Christidis & Marcopoulos, 1995).

LOCATION AND GEOLOGICAL SETTING

The geological characteristics of Milos Island (Fig. 1) have been described by Sonder (1924), Fyticas (1977) and Fyticas *et al.* (1986). The

MATERIALS AND METHODS

Five bentonite samples were collected from the deposits of Ano Komia, Garyfalakena, Mavrogiannis and Rema (Table 1), located in the

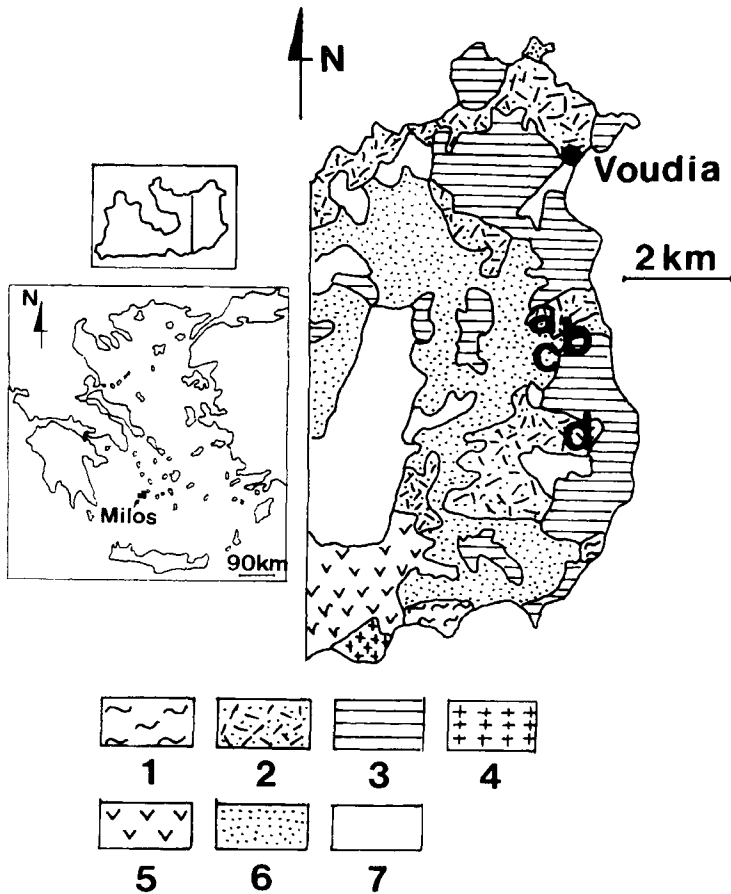


FIG. 1. Simplified geological map of Milos Island (modified after Fyticas *et al.*, 1986). Key to the numbers 1 = metamorphic basement, 2 = pyroclastic rocks (undifferentiated), 3 = lavas (undifferentiated), 4 = lava dome of Halepa, 5 = rhyolitic complex of Phyrliplaka, 6 = chaotic formation ('green lahar' of Fyticas, 1977), 7 = alluvial deposits, f = Ano Komia deposit, h = Garyfalakena deposit, i = Mavrogiannis deposit, j = Rema deposit.

TABLE 1. Mineralogical composition of bentonites. All samples except for SM136 come from the same bentonite horizon.

Mineral phase	Ano Komia		Garyfalakena	Mavrogiannis	Rema
	SM136	SM155	SM163	SM176	SM235
Smectite	M	M	M	M	M
Kaolinite	T	—	T	T	—
Mica	T	—	T	—	—
Opal-CT	—	M	M	M	M
Quartz	M	—	M	M	Min
K-feldspar	Min	Min	M	Min	—
Plagioclase	Min	—	—	—	—
Gypsum	—	—	—	T	—
Pyrite	—	—	T	T	T
Apatite	—	—	—	T	—

M = major mineral phase, Min = minor mineral phase, T = present.

central part of eastern Milos (Fig. 1). Except for SM136, all samples were collected from the same bentonite horizon which extends over a large area. All samples were examined by X-ray diffraction (XRD) for bulk and clay mineralogy with a Philips diffractometer equipped with a PW1710 computerized control unit, operating at 40 kV and 30 mA, using Ni-filtered Cu-K α radiation, with the conditions described by Christidis & Dunham (1993).

Epoxy impregnated polished blocks of the samples were used for microanalyses with a JEOL JXA-8600 Superprobe, using a Link series 1 energy dispersive spectrometer (EDS), with 158 eV resolution at 5.8 keV. The conditions used have been described by Christidis & Dunham (1993). Back-scattered electron images were used to eliminate contamination from Ti and Fe oxides. Both defocused (5 μ m diameter) and focused (<1 μ m wide) beam were used. All selected points were analysed for Si, Ti, Al, Fe, Mn, Mg, Ca, Na and K. With the exception of SM163, a minimum of 20 points were analysed from each sample. The elemental concentrations were automatically corrected for atomic number, adsorption in the sample fluorescence, and dead time, using the Link ZAF-4 computer program. The accuracy, precision and detection limits of the method have been examined by Dunham & Wilkinson (1978). The Ti, when detected, was always associated with Ti oxides and was always subtracted from the total, while Mn was always below the detection limit of the instrument. Analyses with totals <70%, and/or

with more than 4 Si atoms per half unit-cell, due to contamination by opal-CT or fine grained quartz impurities, were discarded, and so were analyses having layer and interlayer charge difference >0.02 c.u. per half unit-cell. The accepted analyses have totals varying between 71.50 and 85.50%. Structural formulae were obtained with the assumptions and cation assignments described by Christidis & Dunham (1993).

RESULTS

X-ray diffraction results

The XRD results are shown in Table 1 and Fig. 2a. All samples contain one or more abundant silica phases, which may be opal-CT or opal-C, and/or quartz. The terminology used to describe the silica polymorphs follows Jones & Segnit (1971). All bentonites also contain abundant dioctahedral smectite associated with plagioclase K-feldspar and subordinate kaolinite. Pyrite occurs sporadically, while mica has been identified in the deposits of Ano Komia and Garyfalakena. The K-feldspar has been characterized as authigenic (Christidis *et al.*, 1995). The XRD results for the orientated clay fractions show (Fig. 2b) that smectite is the main clay mineral phase associated with minor kaolinite in the deposits of Ano Komia and Garyfalakena. Opal-CT is present in most traces suggesting that its size is <2 μ m. The absence of mica from the clay fraction indicates that it is coarse grained and may have been derived from the metamorphic basement.

Microprobe results

Average values of the elements analysed and the cation distributions, standard deviations as well as minimum and maximum values are given in Table 2. The results show that smectites derived from acidic rocks display considerable compositional variation, like their counterparts derived from intermediate precursors (Christidis & Dunham, 1993). However, the characteristics of this variation are different in the two cases.

The relationships between the octahedral cations are shown in Fig. 3. There is a weak negative relationship between Fe^{3+} and octahedral Al ($r = -0.4656$); this relationship is overall and describes the total population (Fig. 3a). Hence, smectites from different deposits plot in different areas of the diagram, although they have been derived from the same precursor. Moreover, no relationship seems to hold in smectites from each individual deposit. A negative relationship ($r = -0.7229$) holds also between Mg and Al^{VI} (Fig. 3b). Again, smectites from different deposits plot in different parts of the diagram. An exception is shown by the smectites from the lower horizon of the Ano Komia deposit (SM136) which cover the entire range. Smectites from SM176 and SM155 are characterized by variation of Mg over a constant Al^{VI} content. Finally no relationship is observed between octahedral Fe and Mg (Fig. 4b).

The weak negative relationship between Fe^{3+} and Al^{VI} is at odds with the well expressed negative relationship observed in smectites derived from intermediate rocks (Christidis & Dunham, 1993). The same holds for the overall character of the variation. It seems that the relative abundance of Fe is not the controlling factor for the compositional variations of these smectites.

Silicon does not seem to be correlated with either Mg or Fe^{3+} (Figs. 3c, 4a). In contrast, a very well expressed negative relationship ($r = -0.9190$) holds between Si and total Al (Fig. 4c). Moreover, the variation observed in each sample suffices to describe the total variation observed. The relationship observed is better expressed in these smectites compared to their counterparts derived from intermediate precursors (Christidis & Dunham, 1993). The relative variation between Al and Si seems to be the most important factor controlling the chemistry of the smectites examined.

Plots between total Al and either tetrahedral or octahedral Al (Fig. 4d,e) show a well expressed

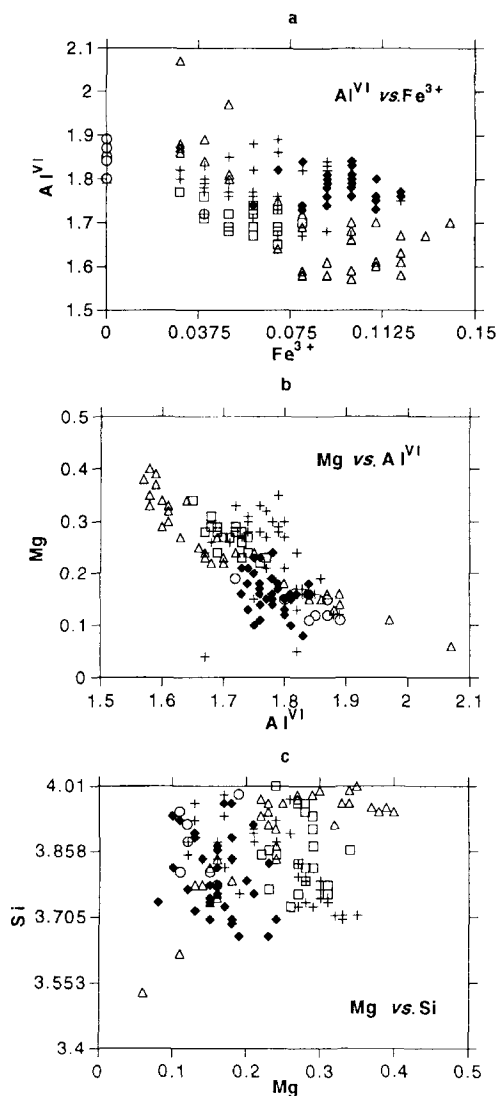


Fig. 3. Orthogonal plots showing the relationship between the octahedral cations in the smectites studied; Al^{VI} stands for octahedral Al. For discussion see text. Δ = SM136; \blacklozenge = SM155; $+$ = SM176; \circ = SM163; \square = SM235.

positive relationship ($r = 0.9190$ and 0.7917 , respectively) corroborating Weaver & Pollard (1973). However, the slope of the straight line in the case of Al^{IV} is much greater compared with Al^{VI} (0.6426 and 0.3574 , respectively). This indicates that with increasing Al content, tetrahedral Al increases at a faster rate than octahedral Al, opposite to the

TABLE 2. Average microanalyses (wt%) and structural formulae of the analysed smectites.

	SM136 (n = 33)			SM155 (n = 37)			SM176 (n = 39)			SM235 (n = 20)			SM163 (n = 8)		
	Mean	sd	min	Mean	sd	min									
SiO ₂	51.37	1.97	68.89	49.64	2.24	64.67	51.58	1.78	55.34	51.91	1.76	54.40	51.69	1.57	55.03
Al ₂ O ₃	20.56	3.55	30.19	21.88	1.26	24.47	22.39	1.30	25.08	21.17	1.20	22.97	21.85	1.73	23.95
Fe ₂ O ₃	1.45	0.56	2.46	1.67	0.23	2.10	1.05	0.39	1.86	1.04	0.23	1.44	0.12	—	0.61
MgO	2.18	0.75	3.55	1.39	0.32	2.08	2.16	0.63	3.12	2.48	0.29	3.11	1.22	0.25	1.65
CaO	0.58	0.15	0.87	0.78	0.23	1.17	0.45	0.21	1.27	0.86	0.26	1.30	1.34	0.11	1.45
Na ₂ O	0.69	0.24	1.21	0.53	0.12	0.78	0.72	0.21	1.18	0.81	0.33	1.41	0.06	—	0.48
K ₂ O	0.46	0.21	1.06	1.00	0.36	1.64	0.58	0.28	1.28	0.90	0.36	1.80	0.86	0.38	1.73
Total	77.10	3.63	86.42	76.50	2.47	82.10	78.48	2.45	83.70	78.91	2.26	81.94	73.14	1.79	79.78
Structural formulae based on 11 oxygens															
Si	3.89	0.12	4.00	3.80	0.09	3.97	3.83	0.09	3.99	3.86	0.08	4.00	3.90	0.09	4.00
Al ^{IV}	0.11	0.12	0.47	0.20	0.09	0.34	0.17	0.09	0.30	0.14	0.08	0.27	0.10	0.09	0.22
Al ^{VI}	1.72	0.13	2.07	1.78	0.03	1.84	1.78	0.06	1.89	1.71	0.03	1.77	1.84	0.05	1.69
Fe ³⁺	0.08	0.03	0.14	0.10	0.01	0.12	0.06	0.02	0.10	0.06	0.01	0.08	0.00	0.01	0.04
Mg	0.25	0.09	0.40	0.16	0.04	0.24	0.24	0.07	0.35	0.27	0.03	0.34	0.14	0.03	0.19
V ^{VI} Cations	2.05	0.03	2.15	2.03	0.04	2.13	2.08	0.04	2.15	2.04	0.02	2.07	1.98	0.03	2.01
Ca	0.05	0.01	0.07	0.06	0.02	0.10	0.03	0.02	0.10	0.05	0.04	0.11	0.11	0.01	0.12
Na	0.09	0.05	0.18	0.03	0.04	0.12	0.06	0.06	0.16	0.11	0.05	0.20	0.01	0.03	0.07
K	0.03	0.02	0.10	0.10	0.03	0.17	0.05	0.03	0.12	0.09	0.03	0.17	0.08	0.04	0.17
L.Charge	0.22	0.06	0.31	0.26	0.07	0.39	0.17	0.08	0.38	0.30	0.04	0.38	0.31	0.04	0.37
I.Charge	0.22	0.06	0.31	0.26	0.07	0.39	0.17	0.08	0.38	0.30	0.04	0.38	0.31	0.04	0.37

n = the number of analysed spots in each sample; sd = standard deviation, max = maximum value, and min = minimum value. L.Charge = layer charge, I.Charge = interlayer charge.

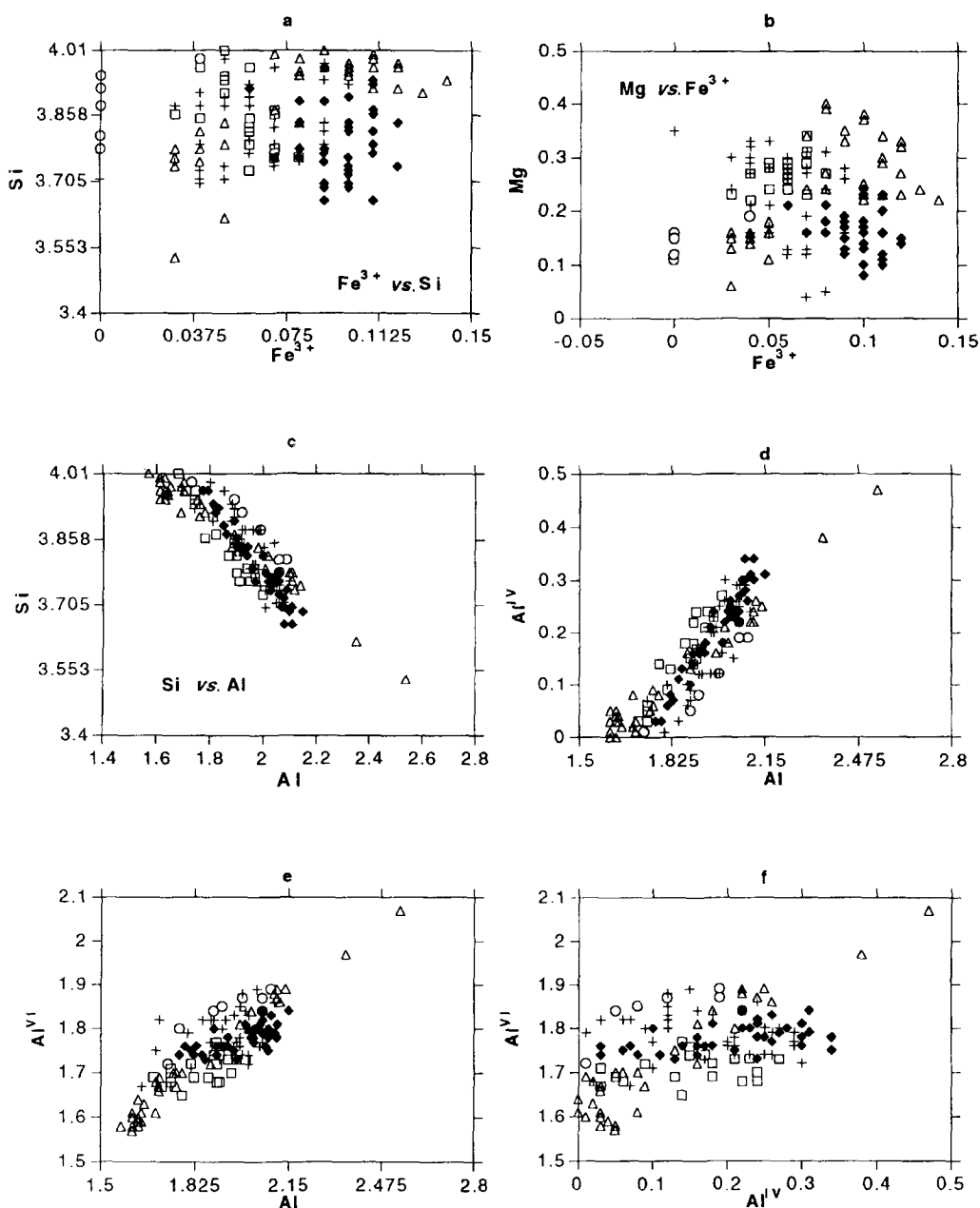


FIG. 4. Orthogonal plots between Fe^{3+} and Si and Fe^{3+} and Mg (a and b respectively), between total Al and Si, Al^{IV} and Al^{VI} (c, d, and e respectively) and between tetrahedral and octahedral Al (f); Al^{IV} and Al^{VI} stand for tetrahedral and octahedral Al respectively. See text for discussion. \triangle = SM136; \blacklozenge = SM155; + = SM176; \circ = SM163; \square = SM235.

findings of Weaver & Pollard (1973). No relationship is observed between octahedral and tetrahedral Al for

all samples except SM136, in which a well defined positive relationship is obvious (Fig. 4f).

A plot of the smectite compositions on the smectite triangle which involves the octahedral cations (Güven, 1988) shows that their composition varies between beidellite and Tatatilla-type montmorillonite (Fig. 5). In SM235 (Rema deposit) mainly Tatatilla-type montmorillonites are present, while smectites from the Garyfalakena deposit (SM163) plot in the field of beidellite. Beidellites are richer in Al and poorer in Fe and Mg than Tatatilla-type montmorillonites, although there is partial overlapping between Al-poor beidellites and Al-rich montmorillonites. Unlike smectites derived from intermediate rocks, no transition towards more Mg-rich smectites (e.g. Chambers-type montmorillonite) is observed. It is obvious that the compositional variation observed in the octahedral sheet is mainly due to the relative abundance of octahedral Al and Mg, while the role of octahedral Fe is minimal.

Layer charge of the smectites

Both beidellite and Tatatilla-type montmorillonite are characterized by layer charge >0.42 c.u. per half unit-cell (Schultz, 1969; Newman & Brown, 1987). The analysed smectites which plot in these fields (Fig. 5) have very low layer charge (Table 2). Moreover, the total number of octahedral cations in many analyses is >2.05 , i.e. the average value quoted by Grim & Güven (1978). Possible reasons for this might be: (a) assumption that all octahedral Fe is present only in the ferric state; (b) assignment of all Mg to octahedral sites; (c) loss of alkalis, especially Na during the microanalyses; (d) existence of hydrogen cations in exchangeable sites; or (e) experimental errors.

The possibility of the presence of ferrous iron in octahedral sites is probably of minor importance, because the Fe content of the analysed smectites is low (see Table 2). Moreover Fe-free smectites are also present. The role of the valence of Fe on the octahedral occupancy might be more important in Wyoming-type and Chambers-type montmorillonites present in the bentonite deposits from Areas 1 and 2 of Milos (Christidis & Dunham, 1993).

The assignment of Mg entirely to octahedral sites might underestimate the amount of interlayer cations. Most beidellites contain almost 2 Al^{VI} atoms per half unit-cell, suggesting that there is no reason to assign all Mg to octahedral sites, especially when small amounts of octahedral Fe

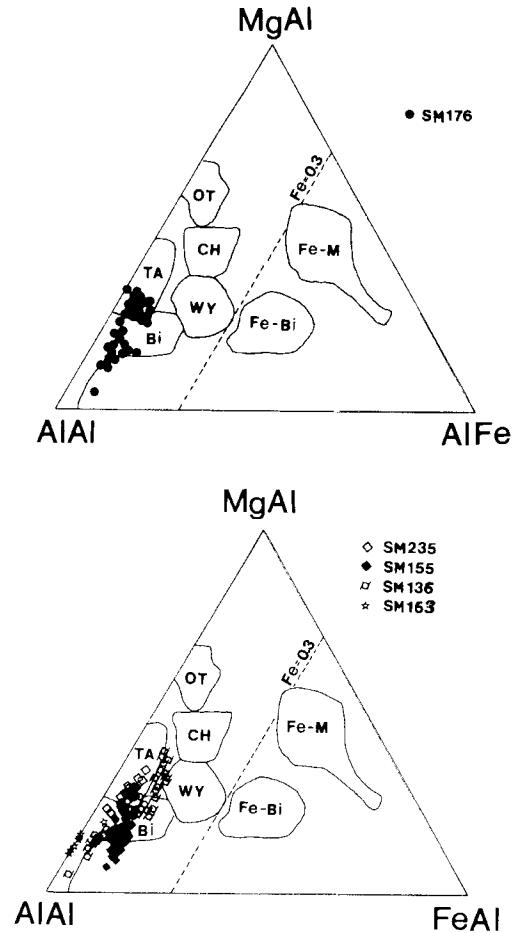


FIG. 5. Projection of smectites in the triangle proposed by Güven (1988). The smectites derived from acidic rocks are projected in the fields of beidellite and Tatatilla-type montmorillonite. See text for discussion. Key to the abbreviations: Bi = beidellite, TA = Tatatilla montmorillonite, CH = Chambers montmorillonite, OT = Otay montmorillonite, WY = Wyoming montmorillonite, Fe-Bi = Fe-rich beidellite, Fe-M = Fe-rich montmorillonite. The dashed line at Fe = 0.3 atoms separates the Fe-rich smectites.

are present. The existence of exchangeable Mg has indirectly been postulated on the basis of some characteristic foundry properties of these bentonites; when untreated they develop high dry compression strength, but low wet tensile strength (Christidis & Scott, 1995). This behaviour is typical of Mg-bearing bentonites (Stephens & Waterworth, 1968).

Christidis (1989) found that in the Garyfalakena deposit Mg, occupies ~70% of the exchangeable sites. Although extraction of Mg from octahedral sites might occur to some extent (Alberti & Brigatti, 1985), it cannot explain such a high Mg content in exchangeable sites. Within the limits of the microprobe analysis the amount of exchangeable Mg cannot be assessed.

Alkalis (especially Na) are very susceptible to loss during microanalysis (Velde, 1984). In the present case, loss of Na has probably taken place, especially when a focused beam was used. The effect of Na loss on the microanalyses has been assessed in Table 3, in which three different sets of data are presented for each sample. Column (a) contains the actual elemental concentrations obtained from each analysis, and the structural formulae derived from it. In column (b) it is assumed that all Na has been lost during the analysis, while in column (c) it is assumed that 1.5% Na₂O is present. Adjustments in other elemental concentrations were not made, because in the ZAF correction, loss of an element is not compensated by an increase in the abundance of the remaining elements, but is presented in the form of

a low total. The results in Table 3 show that loss of Na results in an increase in the total number of octahedral cations and this in turn in an apparent low layer charge. However, the coordinates used in the smectite triangle (Güven, 1988) are hardly affected by this alkali loss, suggesting that the results in Fig. 5 are realistic.

The existence of H⁺ in exchangeable sites might also cause an apparently low interlayer charge, because H⁺ concentration is not determined during microanalyses. However, pH measurements (Christidis, 1992) have shown that there is no reason to expect hydronium concentrations high enough to explain the low interlayer charge values. Finally, experimental errors can explain the observed scattering (clusters of analytical points in Figs. 3,4,5) to some degree but not the well expressed observed trends.

Effect of contamination from fine-grained mineral phases on the structural formulae

The presence of fine-grained Fe oxides or silica-phases in small amounts in the clay fraction might affect the structural formulae determined by

TABLE 3. Effect of loss of alkalis on the microprobe analyses.

Sample	SM136			SM176			SM235		
	a	b	c	a	b	c	a	b	c
Si	3.62	3.63	3.60	3.80	3.81	3.78	3.79	3.81	3.77
Al ^{IV}	0.38	0.37	0.40	0.20	0.19	0.22	0.21	0.19	0.23
Al ^{VI}	1.97	1.99	1.93	1.77	1.79	1.73	1.73	1.75	1.69
Fe ³⁺	0.05	0.05	0.05	0.06	0.06	0.06	0.06	0.06	0.06
Mg	0.11	0.11	0.11	0.27	0.27	0.27	0.28	0.28	0.28
VI cations	2.13	2.15	2.09	2.10	2.12	2.06	2.07	2.10	2.03
Ca	0.00	0.00	0.00	0.03	0.03	0.03	0.07	0.07	0.07
Na	0.06	0.00	0.21	0.08	0.00	0.21	0.11	0.00	0.23
K	0.04	0.04	0.04	0.04	0.04	0.03	0.04	0.04	0.04
Layer charge	0.10	0.04	0.25	0.17	0.10	0.31	0.29	0.20	0.42
Interlayer charge	0.10	0.03	0.25	0.18	0.10	0.30	0.29	0.18	0.41
AlAl	1.85	1.85	1.85	1.68	1.69	1.68	1.67	1.67	1.67
AlMg	0.10	0.10	0.10	0.26	0.25	0.26	0.27	0.27	0.27
AlFe ³⁺	0.04	0.04	0.04	0.06	0.06	0.06	0.06	0.06	0.06

a = actual analysis; b = assumption that all Na has been lost (% Na₂O); c = assumption that 1.5% of Na₂O was originally present in the smectites.

separation of the clay fraction and analysis either with wet geochemical methods or with X-ray fluorescence methods (Warren & Ransom, 1992). For microprobe analysis the sample volume analysed each time is large compared to individual smectite crystallites, the analysed volume depending on the density of the sample and the energy of the electron beam (Potts, 1987). Therefore, a population of an unknown number of smectite crystallites is analysed each time. The use of back-scattered electron images helped to avoid contamination from obvious Fe oxides, Ti oxides or/and silica-phases (especially opal-CT) present on the surface of each sample. Nevertheless, these impurities are not visible if present in close association with smectite crystallites, under the sample surface. In the case of an acidic precursor, the major contaminant is expected to be fine-grained free silica (opal-CT is present). Contamination from free Fe oxides and Ti oxides is less likely, because the Fe content of smectites is low, being comparable to the Fe content of the bentonites (Christidis *et al.*, 1995) and Ti is absent (Table 2).

The effect of contamination from free silica has been estimated in Table 4, to which a beidellite from the Mavrogiannis deposit (column 1), in the

amounts of 1%, 2%, 5%, 10%, and 20% free silica was added. It is obvious that an increase in the degree of contamination results in: (a) a decrease in the tetrahedral charge, as expected; (b) a decrease in the total number of the octahedral cations; and (c) a decrease in the layer charge. Nevertheless, the coordinates used in the smectite triangle (Güven, 1988) remain essentially unchanged and only at 20% contamination (i.e. for analyses which have been discarded because Si is >4 atoms) is there a significant shift of the smectite compositions towards the beidellite corner. Hence, the smectite triangle provides reliable information about the crystal chemical characteristics even at high degrees of Si contamination. On this basis, it is inferred that the smectites from the Garyfalakena deposit have probably been contaminated by Si, because although they plot in the beidellite field (Fig. 5), their tetrahedral charge is small (Table 2).

The possibility of contamination questions the validity of the linear trends between Mg and Al^{VI} (Fig. 3b) and between Si and Al (Fig. 4c). Since the Al^{VI}:Mg ratio does not change in the cases where the number of Si atoms is <4 (Table 4), contamination with up to 10% SiO₂ does not affect the negative trend observed in Fig. 3b.

TABLE 4. Effect of Si contamination on the microprobe analyses of smectites. The analysis in column 1 corresponds to a beidellite from the Mavrogiannis deposit.

	1	1% SiO ₂	2% SiO ₂	5% SiO ₂	10% SiO ₂	20% SiO ₂
Si	3.71	3.73	3.75	3.83	3.93	4.14
Al ^{IV}	0.29	0.27	0.25	0.17	0.07	-0.14
Al ^{VI}	1.77	1.76	1.76	1.76	1.74	1.70
Fe ³⁺	0.04	0.04	0.04	0.03	0.03	0.03
Mg	0.32	0.32	0.31	0.30	0.28	0.24
^{VI} cations	2.13	2.12	2.11	2.08	2.05	1.97
Ca	0.02	0.02	0.02	0.02	0.02	0.02
Na	0.16	0.16	0.16	0.13	0.13	0.12
K	0.04	0.04	0.03	0.03	0.03	0.03
Layer charge	0.22	0.23	0.23	0.20	0.20	0.13
Interlayer charge	0.24	0.24	0.23	0.22	0.20	0.19
AlAl	1.67	1.67	1.67	1.68	1.69	1.72
AlFe ³⁺	0.03	0.03	0.03	0.03	0.03	0.03
AlMg	0.30	0.30	0.30	0.29	0.28	0.25

However, the Si:Al ratio increases with increasing degree of contamination (Table 4). In Fig. 6 the two regression lines corresponding to the analysed smectites (line a) and the contaminated beidellite (line b) are very close. Hence the negative linear relationship between Si and Al might be considered, at least to a degree, as an artifact.

Contamination by Si results in a reduction in Al^{IV} , leaving Al^{VI} and Mg essentially unchanged (Table 4). In Fig. 7a, Si is plotted with Al^{VI} and Mg. An increase in the Si content of smectites is associated with an increase of the Al^{VI} and a sharp decrease of the Mg content. The Si/ Al^{VI} ratio of the Si-poor smectites (i.e. Mg-rich end) is greater than the Si-rich smectites. In Fig. 7b, the Si contaminated beidellite is plotted with the same coordinates. A comparison with Fig. 7a shows that: (i) the direction of the compositional trends is significantly different; (ii) the Si/ Al^{VI} ratio increases with increasing degree of contamination; and (iii) the spread of the values obtained is much smaller than that of the smectite population. Therefore, it is believed that Si contamination is not the main reason for the variation observed and that this variation is not an artifact. Nevertheless it might cause scattering, in a direction parallel to the Mg-Si line.

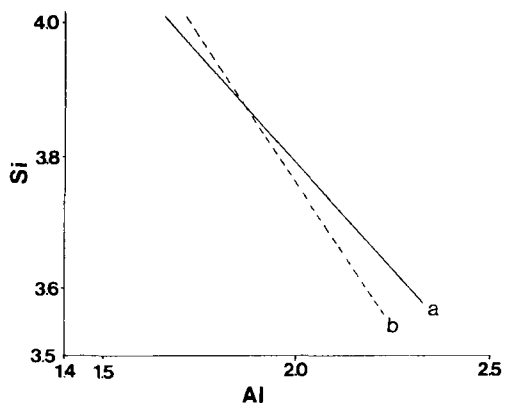


FIG. 6. Effect of contamination by Si on the microanalytical data. The solid line (a) corresponds to the regression line in Fig. 4c, while the dashed line (b) was constructed using a beidellite contaminated with various amounts of Si. See text for discussion.

Back-scattered electron images

Back-scattered electron images of SM136 and SM176 (Fig. 8) coupled with microanalyses in SM136 using a focused beam revealed the existence of zonation in smectite composition, from the rims towards the interior of the altered shards (Table 5).

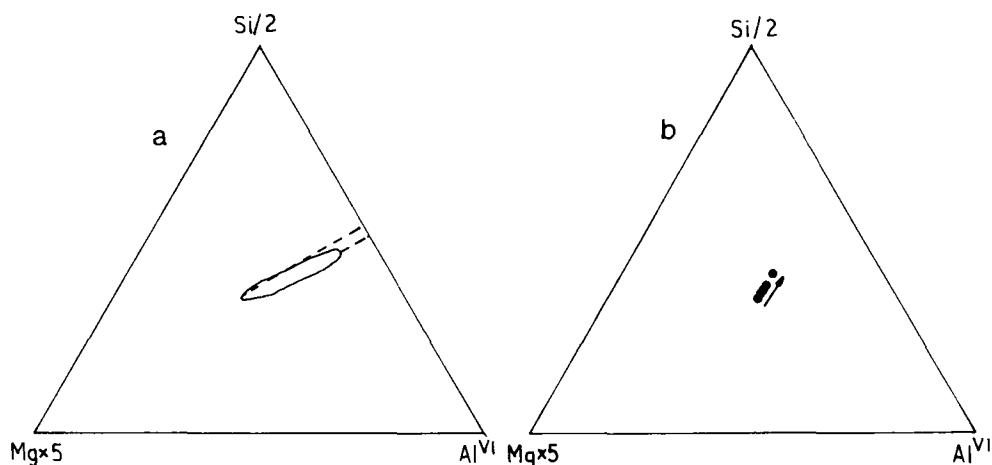


FIG. 7. Evaluation of contamination by Si using the main structural cations of the smectites derived from acidic rocks (Si, Al^{VI} , Mg): (a) actual population, (b) beidellites contaminated with various amounts of Si. The dashed line shows the limits of scattering. Note the different trends displayed in the two diagrams. See text for discussion.

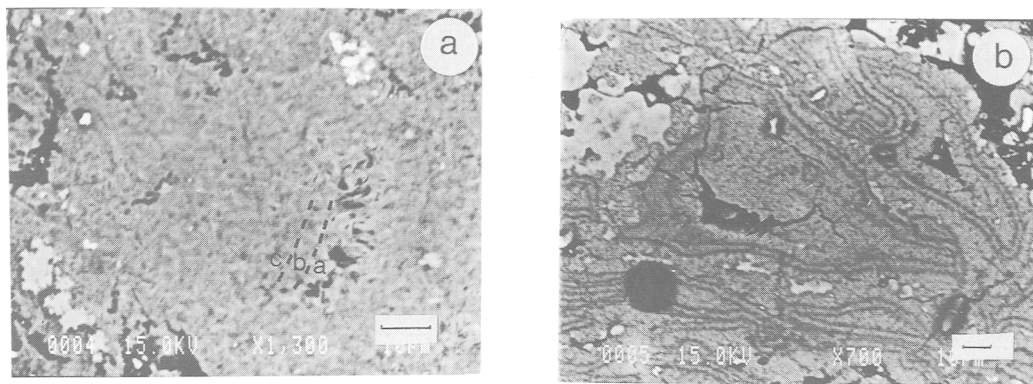


FIG. 8. Back-scattered electron images characteristic of the bentonite studied. (a) SM135 (Ano Komia deposit). The dashed lines divide three zones with different smectite composition: zone (a) contains beidellite with variable composition, zone (b) contains Tatatilla-type montmorillonite, while in zone (c) free opal-CT has precipitated. The bright grains at the top of the photograph and those disseminated in the fine-grained mass belong to pyrite, while the dull, greyish-white, fine-grained material, close to the lower left-hand corner belongs to opal-CT. The bright elongated crystal in the lower left-hand corner belongs to authigenic K-feldspar. (b) SM176 (Mavrogiannis deposit). Concentric layers of opal-CT probably on smectite flakes. The greyish-white material belongs also to opal-CT. Scale bars 10 μ m.

In Fig. 8a, zone (a) consists of beidellite with variable composition (analyses 1–3 in Table 5), zone (b) consists of Tatatilla-type montmorillonite (analyses 4,5) while in zone (c) free silica has precipitated (analysis 6). The principal chemical factor controlling the zoned composition of smectites is the Si:Al ratio, in good agreement with Fig. 4c. The beidellite zone is also poor in Fe and Mg compared to the montmorillonite zone. The morphological characteristics of the smectites are different in the three zones; in zone (a) well-formed beidellite crystallites are present, their size decreasing towards the interior of the shards. The released silica has precipitated either in pore cavities formed from the dissolution of the glass, or in the form of concentric layers (Fig. 8b), probably on smectite flakes.

DISCUSSION

Compositional characteristics of smectites

The chemical characteristics which control the compositional variations of smectites are different in different smectite types derived from intermediate rocks (Christidis & Dunham, 1993). Similar patterns are observed in smectites derived

from acidic rocks (Fig. 9). This indicates that different mechanisms control the formation of the different types of smectites. In montmorillonites, an increase of Mg is accompanied by a decrease of both Fe and Al^{VI}. In beidellites, the compositional patterns are different in different samples; in SM136 an increase of Mg is accompanied by a concomitant increase of Fe and the Fe³⁺:Al^{VI} ratio, while in SM176 and SM155 an increase of Mg is associated with a decrease in Fe. However, the Fe³⁺:Al^{VI} ratio increases (SM155) or remains constant (SM176) because of the simultaneous decrease in the Al^{VI} content. Also, an increase in the Si content in all smectites is accompanied by a decrease in the Fe content and concomitant increase in the Al^{VI} content (Fig. 9).

The smectites in the bentonites studied are Al-rich, with compositions ranging between beidellite and Tatatilla-type montmorillonite (Fig. 5). The transition is continuous suggesting the possibility of a solid-solution between them. A similar transition has been observed in smectites derived from intermediate rocks (Christidis & Dunham, 1993). Since beidellites and Tatatilla-type montmorillonites differ mainly in the distribution of the layer charge (see Güven, 1988), there is no reason to exclude the possibility of a solid-solution between

TABLE 5. Compositional variation of smectites across an altered glass shard from the Ano Komia deposit (see Fig. 8a). Analyses 1, 2 and 3 come from zone (a) and belong to beidellites; analyses 4 and 5 come from zone (b) (Fig. 8b) and belong to Tatatilla montmorillonites; and analysis 6 comes from zone (c) and corresponds to smectites closely intergrown with a fine grained free silica phase (opal-CT).

	Zone a			Zone b		Zone C
	1	2	3	4	5	6
SiO ₂	49.39	54.00	50.94	48.85	49.69	56.79
Al ₂ O ₃	30.19	25.62	28.04	18.68	19.14	19.85
Fe ₂ O ₃	0.49	0.72	0.86	2.21	1.81	1.48
MgO	0.55	1.31	1.04	1.99	1.99	0.49
CaO	0.26	0.71	—	0.62	0.87	—
Na ₂ O	—	—	0.44	0.68	0.41	—
K ₂ O	0.35	0.81	0.44	—	—	0.68
Total	81.23	83.17	81.76	73.03	73.91	79.29
Structural formulae based on 11 oxygens						
Si	3.53	3.78	3.62	3.91	3.92	4.12
Al ^{IV}	0.47	0.22	0.38	0.09	0.08	-0.12
Al ^{VI}	2.07	1.89	1.97	1.67	1.69	1.82
Fe ³⁺	0.03	0.04	0.05	0.13	0.11	0.08
Mg	0.06	0.14	0.11	0.24	0.23	0.05
VI cations	2.16	2.07	2.13	2.04	2.03	1.96
Ca	0.02	0.05	0.00	0.05	0.07	0.00
Na	0.00	0.00	0.06	0.11	0.06	0.00
K	0.03	0.07	0.04	0.00	0.00	0.06
AlAl	1.92	1.83	1.85	1.64	1.66	1.86
AlMg	0.05	0.13	0.11	0.23	0.23	0.05
AlFe ³⁺	0.03	0.04	0.04	0.13	0.11	0.09

these two species. The alternative possibility is to assume the existence of two domains, one with beidellitic and one with montmorillonitic (Tatatilla-type montmorillonite) composition (Decarreau *et al.*, 1987). This assumption is based on the fact that in each microanalysis an unknown population of smectite crystals is analysed, and requires a linear distribution of the smectite compositions between the two end-members.

In Fig. 10, Al^{IV} is plotted with Al^{VI} and Mg, the most important parameters controlling the chemistry of beidellites and Al-rich montmorillonites. The compositional variation of both beidellite and (especially) montmorillonite is broad and too complex to be explained by mixtures of two domains having different composition, unless the end-member composition of these domains varies between broad limits. Also, the compositional

transitions in different samples follow different trends (Fig. 10b). Thus, even if mechanical mixtures are the reason for the observed compositional variation, it is certain that the microenvironmental conditions during the formation of the bentonite were different at different parts of the parent rock. Detailed work with other microbeam techniques such as AEM might help to clarify this point, as has been shown for other authigenic clay minerals (Warren & Curtis, 1989).

Alteration of an acidic rock to bentonite

Dissolution of acidic volcanic glass produces smectites only when the pore fluid acts as a sink, i.e. when the system is well flushed (Dibble & Tiller, 1981). In closed systems, alkali zeolites are formed because they are favoured by high

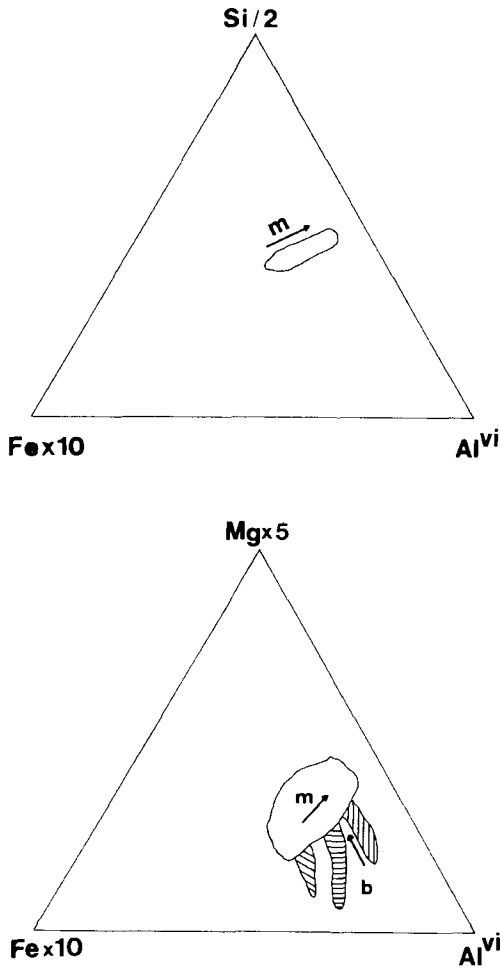


FIG. 9. Triangular diagrams showing the chemical characteristics which control the compositional variations of smectites derived from acidic rocks. The empty fields correspond to montmorillonite (m), and the hatched fields to beidellite (b). Vertical hatching: SM136, oblique hatching: SM155, horizontal hatching: SM176. See text for discussion.

($\text{Na}^+ + \text{K}^+$)/ H^+ activity ratios (Hess, 1966). In such systems smectite is formed during the initial stages of alteration (c.f. Sheppard & Gude, 1973; Dibble & Tiller, 1981; Hay & Goldman, 1987), in which salinity and alkalinity are probably low (Sheppard & Gude, 1973). The lack of zeolites and the large scale of Si migration from the rims of the glass shards (formation of beidellite in Fig. 8a), indicates the existence of a well-flushed system during alteration of the volcanic glass.

The Al_2O_3 content of beidellites in the rim of the altered shards (Fig. 8a, Table 5) is, in places, more than twice the average rhyolite composition (Fisher & Schmincke, 1984). This enrichment is residual because Al is immobile under the pH conditions (submarine environment) prevailing during alteration (White, 1983). Magnesium probably displays a short-range redistribution in the rims of the shards, because the $\text{MgO}:\text{Al}_2\text{O}_3$ ratio of some beidellite crystallites (analysis 1 in Table 5) is much lower than that of the average rhyolite (Fischer & Schmincke, 1984) while in others it is much higher (analysis 2 in Table 5). Hence, even in the case of an acidic rock, alteration to bentonite is not necessarily accompanied by uptake of Mg from the pore fluid as previously thought (e.g. Zielinski, 1982; Shiraki *et al.*, 1987), at least in places. The increase in the Mg content in zone b (Fig. 8) is not residual because the $\text{MgO}:\text{Al}_2\text{O}_3$ ratio of smectites is much higher than the average rhyolite. In this instance, Mg has probably been provided by sea water.

The Fe also seems to be mobile during the alteration, suggesting a low oxygen fugacity. Migration of Fe has taken place from the beidellite-rich zone. In zone b (Fig. 8a), it is not certain whether Fe has behaved residually or has migrated. This is because, although the Fe content of these smectites is lower than the average rhyolite, similar parent rocks of some bentonites from Kimolos Island have very low Fe contents (Christidis, 1996). If the parent rocks had low Fe content, then Fe has not migrated from zone (b). In this case even redistribution of Fe released from zone (a) should be considered.

The small-scale zonation of the smectite composition and the compositional variation in smectite chemistry underlines the importance of microenvironmental chemistry, largely controlled by the composition of the fluid phase during the formation of smectites, similar to smectites derived from intermediate rocks (Christidis & Dunham, 1993). This is supported by the different Fe and Mg contents of the smectites in the different samples (Figs. 3,4,5), although they were derived from a common precursor. The role of the fluid phase for the chemical variability of clay minerals has been recognized in the past (Tardy *et al.*, 1982) and has been discussed in weathering profiles (Paquet *et al.*, 1982; Banfield & Eggleton, 1990), but data on bentonites are limited. Two alternative explanations for this variation are: (i) the existence of mixtures

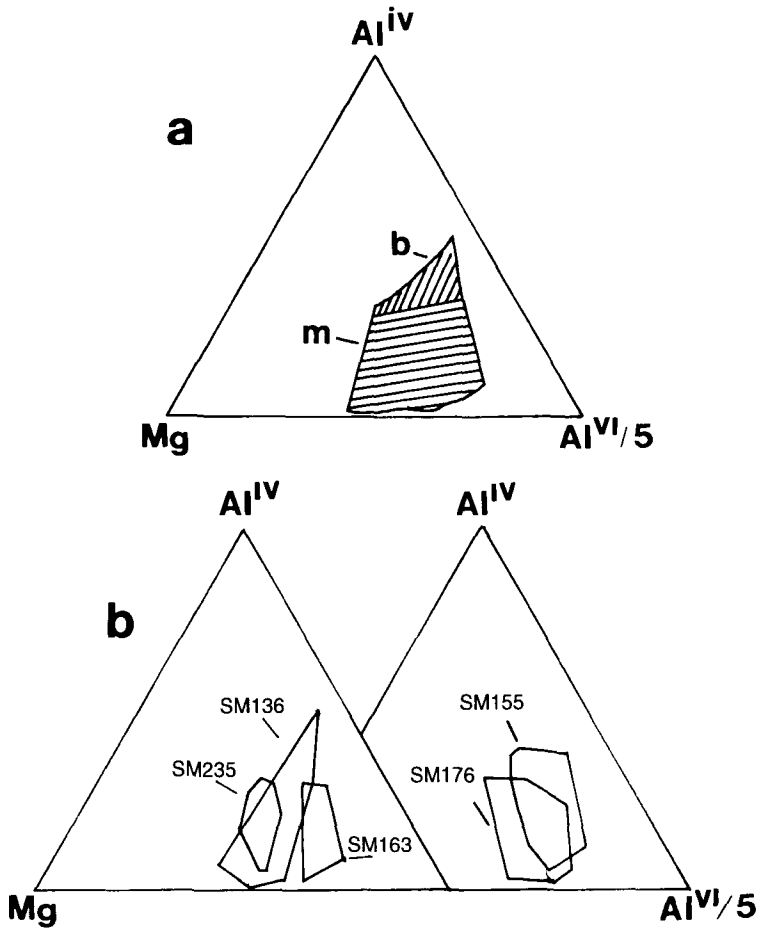


FIG. 10. Projection of smectites in triangular diagrams using the most important elements which describe their composition; (a) compositional ranges of the overall smectite population, b = beidellites, m = montmorillonites; (b) compositional ranges for each individual sample. See text for discussion.

between compositionally distinct domains discussed before; and (ii) inhomogeneity of the parent glass. So far, little is known about the inhomogeneity of natural glasses. However, such an assumption cannot explain the large variation in the $Al_2O_3:SiO_2$ ratio observed, expressed with the existence of beidellite in the rim and Tatatilla-type montmorillonite in the interior of the glass shards.

The compositional characteristics of smectites are also affected by the nature of the parent rock. Thus, the role of Fe is rather limited, in contrast to smectites derived from intermediate rocks (Christidis & Dunham, 1993). On the other hand, the relative abundances of Si and Al (caused by the

variable degree of Si release) and to a lesser degree Mg (caused by microscale migration and/or different degree of uptake from the sea water) are of major importance. These chemical characteristics are reflected on the crystal chemistry of the smectites formed from the acidic rocks in the Komia area, Milos; beidellites and Tatatilla-type montmorillonites are present, while Wyoming-type or Chambers-type montmorillonites, are absent. However, in some instances the role of the pore fluid might overprint the parent rock signature (e.g. Christidis, 1996).

Alteration of acidic rocks to bentonites releases large amounts of silica because the Si:Al ratio of

smectites is much lower than the parent rock, especially for beidellite. In this study, the excess silica precipitates within the bentonite in the form of opal-CT. The downward migration of free silica mentioned by Grim & Güven (1978) was not observed. The precipitation of opal-CT effectively dilutes the smectite content of bentonites. Since opal-CT is finer than 2 μm and is closely associated with smectites (Fig. 8), it probably adversely affects the physical properties of bentonites (Christidis & Scott, 1995). Therefore, unless the excess silica is removed (e.g. Zielinski, 1982; Christidis, 1996) acidic precursors are not expected to form good quality bentonites. Also, the formation of smectites with predominantly tetrahedral layer charge (i.e. beidellites) from acidic precursors, might affect properties such as swelling (Suquet *et al.*, 1975) which is related to the rheological characteristics of bentonites (Callaghan & Ottewill, 1974; Rand *et al.*, 1980).

CONCLUSIONS

The smectites derived from acidic precursors in Milos Island, Greece, display significant compositional variations between beidellite and Tatatilla-type montmorillonite. Alkali loss and contamination by fine-grained phases, like opal-CT, affect the cation distribution in the structural formulae and might provide misleading information about the nature of smectite. The problem can be overcome by the use of suitable diagrams for projection of smectites, such as the diagram proposed by Güven (1988), which is hardly affected by these factors. Although the compositional transition is continuous, it is not certain whether there is a solid-solution between beidellite and Tatatilla-type montmorillonite or whether the variation observed is due to mechanical mixing of domains with different composition.

The type of smectite formed depends on the nature of the parent rock which induces an inherited factor in the form of limited Fe content and the fluid chemistry. Wyoming-type montmorillonites are not expected to form from acidic precursors, unless Fe and Mg are supplied by the fluid phase. Acidic rocks favour the formation of beidellite and Tatatilla-type montmorillonite. Such rocks are not suitable precursors for high quality bentonites because the large amount of Si released during the alteration precipitates in the form of opal-CT in the bentonites. Finally, although Mg uptake is an

important characteristic of bentonite formation, under certain conditions redistribution of Mg rather than uptake of Mg takes place.

ACKNOWLEDGMENTS

This work is part of the PhD project of GC which was financially supported by the Greek State Scholarship Foundation (SSF). The constructive comments of two anonymous reviewers and the editor improved the text. We are grateful to the Silver and Barytes Ore Mining Co., Greece for their permission for sample collection from their quarries.

REFERENCES

- Alberti A. & Brigatti M.F. (1985) Crystal chemical differences in Al-rich smectites as shown by multivariate analysis of variance and discriminant analysis. *Clays Clay Miner.* **33**, 546–558.
- Banfield J.F. & Eggleton R.A. (1990) Analytical transmission electron microscope studies of plagioclase, muscovite, and K-feldspar weathering. *Clays Clay Miner.* **38**, 77–89.
- Banfield J.F., Jones B.R. & Veblen D.R. (1991a) An AEM-TEM study of weathering and diagenesis, Albert Lake, Oregon: I. Weathering reactions in the volcanics. *Geochim. Cosmochim. Acta*, **55**, 2781–2793.
- Banfield J.F., Jones B.R. & Veblen D.R. (1991b) An AEM-TEM study of weathering and diagenesis, Albert Lake, Oregon. II. Diagenetic modification of the sedimentary assemblage. *Geochim. Cosmochim. Acta*, **55**, 2795–2810.
- Brigatti M.F. & Poppi L. (1981) A mathematical model to distinguish the members of the dioctahedral smectite series. *Clay Miner.* **16**, 81–89.
- Callaghan I.C. & Ottewill R.H. (1974) Interparticle forces in montmorillonite gels. *Disc. Faraday Soc.* **57**, 597–606.
- Christidis G. (1989) *Mineralogy, physical and chemical properties of the bentonite deposits of Milos island, Greece*. MSc thesis, Univ. Hull, UK.
- Christidis G. (1992) *Origin, and physical and chemical properties of the bentonite deposits from the Aegean islands of Milos, Kimolos, and Chios, Greece*. PhD thesis, Univ. Leicester, UK.
- Christidis G. (1996) Formation and recrystallization through Ostwald ripening of smectites from Kimolos Island, Aegean, Greece. Submitted to *Am. Miner.*
- Christidis G. & Dunham A.C. (1993) Compositional variations in smectites Part I. Alteration of intermediate volcanic rocks. A case study from Milos Island, Greece. *Clay Miner.* **28**, 255–273.
- Christidis G. & Marcopoulos T. (1995) Mechanism of formation of kaolinite and halloysite in the bentonite

- deposits of Milos Island, Greece. *Chem. Erde*, **55**, 315–329.
- Christidis G. & Scott P.W. (1995) Physical and chemical properties of the bentonite deposits of Milos Island, Greece. *Trans. IMM* (in press).
- Christidis G., Scott P.W. & Marcopoulos T. (1995) Origin of the bentonite deposits of Eastern Milos, Aegean, Greece: Geological, Mineralogical and Geochemical evidence. *Clays Clay Miner.* **43**, 63–77.
- Decarreau A., Colin F., Herbillon A., Manceau A., Nahon D., Paquet H., Trauth-Badeaud D. & Trescases J.J. (1987) Domain segregation in Ni-Fe-Mg-smectites. *Clays Clay Miner.* **35**, 1–10.
- Dibble W.E. Jr & Tiller W. (1981) Kinetic model of zeolite paragenesis in tuffaceous sediments. *Clays Clay Miner.* **29**, 323–330.
- Dunham A.C. & Wilkinson F.C.F. (1978) Accuracy, precision and detection limits of Energy Dispersive Electron-microprobe analyses of silicates. *X-ray Spectrometry*, **7**, 50–56.
- Fisher R.V. & Schmincke H.U. (1984) *Pyroclastic Rocks*, pp. 11–34. Springer Verlag, Berlin.
- Fyticas M. (1977) *Geological and geothermal study of Milos island*. PhD thesis, Univ. Salonica, Greece.
- Fyticas M., Innocenti F., Kolios N., Manetti P., Mazzuoli R., Poli G., Rita F. & Villari L. (1986) Volcanology and petrology of volcanic products from the island of Milos and neighbouring islets. *J. Volcanol. Geotherm. Res.* **28**, 297–317.
- Goodman B.A., Nadeau P.H. & Chadwick J. (1988) Evidence for the multiphase nature of bentonites from Mossbauer and EPR spectroscopy. *Clay Miner.* **23**, 147–159.
- Goulding K.W.T. & Talibudeen O. (1980) Heterogeneity of cation-exchange sites for K-Ca exchange in aluminosilicates. *J. Coll. Interf. Sci.* **78**, 15–24.
- Grim R.E. & Kulbicki G. (1961) Montmorillonite: High temperature reactions and classification. *Am. Miner.* **46**, 1329–1369.
- Grim R.E. & Güven N. (1978) *Bentonites. Geology, Mineralogy, Properties and Uses*, pp. 143–155. Elsevier, Amsterdam.
- Güven N. (1988) Smectite. Pp. 497–559 in: *Hydrous Phyllosilicates* (S.W. Bailey, editor). Reviews in Mineralogy, Vol. **19**. Mineralogical Society of America, Washington, DC.
- Hay R.L. & Guldman S.G. (1987) Diagenetic alteration of silicic ash in Searles lake, California. *Clays Clay Miner.* **35**, 449–457.
- Hess P.C. (1966) Phase equilibria of some minerals in the $K_2O-Na_2O-Al_2O_3-SiO_2-H_2O$ system at 25°C and 1 atmosphere. *Am. J. Sci.* **264**, 289–309.
- Iwazaki T. & Watanabe T. (1988) Distribution of Ca and Na ions in dioctahedral smectites and interstratified dioctahedral mica/smectites. *Clays Clay Miner.* **36**, 73–82.
- Jones J.B. & Segnit E.R. (1971) The nature of opal. I Nomenclature and constituent phases. *J. Geol. Soc. Australia*, **18**, 57–68.
- Köster H.M. (1982) The crystal structure of 2:1 Layer silicates. *Proc. Int. Clay Conf., Bologna-Pavia*, 41–71.
- Lagaly G. & Weiss A. (1975) The layer charge of smectitic layer silicates. *Proc. Int. Clay Conf. Mexico*, 157–172.
- Lagaly G., Fernandez-Gonzalez M. & Weiss A. (1976) Problems in layer-charge determination of montmorillonites. *Clay Miner.* **11**, 173–187.
- Lim C.H. & Jackson M.L. (1986) Expandable phyllosilicate reactions with lithium on heating. *Clays Clay Miner.* **34**, 346–352.
- Meunier A. & Velde B. (1989) Solid-solutions in I/S mixed layer minerals and illite. *Am. Miner.* **74**, 1106–1112.
- Nadeau P.H., Farmer V.C., McHardy W.J. & Bain D.C. (1985) Compositional variations of the Unterrupsthal beidellite. *Am. Miner.* **70**, 1004–1010.
- Newman A.C.D. & Brown G. (1987) The chemical constitution of clays. Pp. 1–128 in: *Chemistry of Clays and Clay Minerals* (A.C.D Newman, editor). Mineralogical Society, London.
- Paquet H., Duplay J. & Nahon D. (1982) Variations in the composition of phyllosilicates monoparticles in a weathering profile of ultrabasic rocks. *Proc. Int. Clay Conf., Bologna-Pavia*, 595–603.
- Potts P.J.A. (1987) *A Handbook of Silicate Rock Analysis*. Blackie & Son, Glasgow & London.
- Rand B., Pekenc, R., Goodwin J.W. & Smith R.B. (1980) Investigation into the existence of edge-face coagulated structures in Na-montmorillonite suspensions. *J. Chem. Soc. Faraday Trans.* **76**, 225–235.
- Schultz L.G. (1969) Lithium and potassium adsorption, dehydroxylation temperature and structural water content of aluminous smectites. *Clays Clay Miner.* **17**, 115–149.
- Sheppard R.A. & Gude 3rd A.J. (1973) Zeolites and associated authigenic silicate minerals in tuffaceous rocks of the Big Sandy Formation, Mohave County, Arizona. *U.S. Geol. Surv. Prof. Paper*, No. **830**, 36pp.
- Shiraki R., Sakai H., Endoh M. & Kishima N. (1987) Experimental studies on rhyolite-and andesite-sea-water interactions at 300°C and 1000 bars. *Geochem. J.* **21**, 139–148.
- Sonder R.A. (1924/25) Zur Geologie und Petrographie der Inselgruppe von Milos. *Z. Volcanologie*, **8**, 181–237.
- Stephens H.A. & Waterworth A.N. (1968) Significance of the exchangeable cation in foundry bentonite. *Brit. Found.* **61**, 202–219.
- Stul M.S. & Mortier W.J. (1974) The heterogeneity of the charge density in montmorillonites. *Clays Clay*

- Miner.* **22**, 391–396.
- Suquet H., de la Calle C. & Pezerat H. (1975) Swelling and structural organization of saponite. *Clays Clay Miner.* **23**, 1–9.
- Talibudeen O. & Goulding K.W.T. (1983) Charge heterogeneity in smectites. *Clays Clay Miner.* **31**, 37–42.
- Tardy Y., Duplay J. & Fritz B. (1982) Chemical composition of individual clay particles: An ideal solid-solution model. *Proc. Int. Clay Conf., Bologna-Pavia*, 441–450.
- Tettenhorst R. & Johns W.D. (1966) Interstratification in montmorillonite. *Clays Clay Miner.* **25**, 85–93.
- Velde B. (1984) Electron microprobe analysis of clay minerals. *Clay Miner.* **19**, 243–247.
- Warren E.A. & Curtis C.D. (1989) The chemical composition of authigenic illite within two sandstone reservoirs as analysed by ATEM. *Clay Miner.* **24**, 137–156.
- Warren E.A. & Ransom B. (1992). The influence of analytical error upon the interpretation of chemical variations in clay minerals. *Clay Miner.* **27**, 193–209.
- Weaver C.E. & Pollard L.D. (1973) *The Chemistry of Clay Minerals*, pp. 55–77. Elsevier, Amsterdam.
- White A.F. (1983) Surface chemistry and dissolution kinetics of glassy rocks at 25°C. *Geochim. Cosmochim. Acta*, **47**, 805–815.
- Yamada H., Nakazawa H., Yoshioka K. & Fujita T. (1991) Smectites in the montmorillonite-beidellite series. *Clay Miner.* **26**, 359–369.
- Zielinski R.A. (1982) The mobility of uranium and other elements during alteration of rhyolite ash to montmorillonite: A case study in the troublesome formation, Colorado, USA. *Chem. Geol.* **35**, 185–204.